Molecular Neurobiology (2022) 59:574–589
https://doi.org/10.1007/s12035-021-02621-5

Phosphodiesterase 10A Is a Critical Target for Neuroprotection in a Mouse Model of Ischemic Stroke

Mustafa C. Beker[1,2] · Ahmet B. Caglayan[2,3] · Serdar Altunay[1,2] · Elif Ozbay[1,2] · Nilay Ates[1,2] · Taha Kelestemur[1,2] · Berrak Caglayan[2,4] · Ulkan Kilic[5] · Thorsten R. Doeppner[6] · Dirk M. Hermann[7] · Ertugrul Kilic[1,2]

Received: 6 May 2021 / Accepted: 26 October 2021 / Published online: 4 November 2021

Abstract

Phosphodiesterase 10A (PDE10A) hydrolyzes adenosine 3′,5′-cyclic monophosphate (cAMP) and guanosine 3′,5′-cyclic monophosphate (cGMP). It is highly expressed in the striatum. Recent evidence implied that PDE10A may be involved in the inflammatory processes following injury, such as ischemic stroke. Its role in ischemic injury was unknown. Herein, we exposed mice to 90 or 30-min middle cerebral artery occlusion, followed by the delivery of the highly selective PDE10A inhibitor TAK-063 (0.3 mg/kg or 3 mg/kg) immediately after reperfusion. Animals were sacrificed after 24 or 72 h, respectively. Both TAK-063 doses enhanced neurological function, reduced infarct volume, increased neuronal survival, reduced brain edema, and increased blood–brain barrier integrity, alongside cerebral microcirculation improvements. Post-ischemic neuroprotection was associated with increased phosphorylation (i.e., activation) of pro-survival Akt, Erk-1/2, GSK-3α/β and anti-apoptotic Bcl-xL abundance, decreased phosphorylation of pro-survival mTOR, and HIF-1α, MMP-9 and pro-apoptotic Bax abundance. Interestingly, PDE10A inhibition reduced inflammatory cytokines/chemokines, including IFN-γ and TNF-α, analyzed by planar surface immunoassay. In addition, liquid chromatography-tandem mass spectrometry revealed 40 proteins were significantly altered by TAK-063. Our study established PDE10A as a target for ischemic stroke therapy.

Keywords cAMP · Focal cerebral ischemia · Inflammation · PDE10A · Phosphodiesterase · TAK-063

Introduction

Phosphodiesterase 10A (PDE10A) is a dual-substrate specific enzyme and an essential regulator of cell signaling by hydrolyzing the second messengers cyclic adenosine monophosphate (cAMP) and cyclic guanosine monophosphate (cGMP) [1, 2], which play crucial roles in neuronal activity, synaptic plasticity, neurogenesis, and apoptosis in the central nervous system (CNS) [3, 4]. In the CNS, PDE10A is highly expressed in medium spiny neurons (MSNs), which make up approximately 95% of all striatal neurons. Through degradation of cAMP and cGMP, PDE10A regulates MSN excitability [5]. Inhibition of PDE10A increases cyclic nucleotide levels and activates its downstream signal transduction pathways including cAMP/protein kinase A (PKA) signaling [4, 6, 7]. The cAMP/PKA signaling pathway regulates many important cellular processes such as cellular proliferation, differentiation, and apoptosis.

In the striatum of transgenic mice developing Huntington's disease pathology, PDE10A protein and mRNA levels

✉ Mustafa C. Beker
mcbeker@medipol.edu.tr

1 Department of Physiology, School of Medicine, Istanbul Medipol University, Istanbul, Turkey

2 Regenerative and Restorative Medical Research Center (REMER), Research Institute for Health Sciences and Technologies (SABITA), Istanbul Medipol University, Istanbul, Turkey

3 Department of Physiology, International School of Medicine, Istanbul Medipol University, Istanbul, Turkey

4 Department of Medical Genetics, International School of Medicine, Istanbul Medipol University, Istanbul, Turkey

5 Department of Medical Biology, International School of Medicine, University of Health Sciences Turkey, Istanbul, Turkey

6 Department of Neurology, University Medicine Göttingen, University of Göttingen, Göttingen, Germany

7 Department of Neurology, University Hospital Essen, University of Duisburg-Essen, Essen, Germany

were found to be decreased prior to the onset of motor symptoms [8]. Again, in mice with Huntington's disease pathology, pharmacological PDE10A inhibition reduced striatal and cortical cell loss, the formation of striatal neuronal intranuclear inclusions, and microglial activation [9]. In a mouse model of Parkinson's disease, PDE10A inhibition increased neuronal survival and decreased microglial activation via cAMP/PKA signaling [10].

Due to its distribution pattern in the striatum where it contributes to the control of movement and cognition, PDE10A has been suggested to be a target for the treatment of neurodegenerative disorders. Indeed, RNA-sequencing transcriptome analysis revealed reduced expression of Adora2a (adenosine receptor A2A), Drd2 (dopamine receptor D2), and Pde10a in spontaneously recovered mice after ischemic stroke [11]. Very recently, Birjandi et al. showed that pharmacological deactivation of PDE10A improved motor recovery after striatal but not cortical ischemic injury, which was associated with increased axonal neuroplasticity and elevated brain-derived neurotrophic factor (BDNF) levels [12]. In this study, the PDE10A inhibitor was administered in the post-acute stroke phase, starting 5 days post stroke. Structural neuroprotective effects of PDE10A inhibition were not studied.

TAK-063 [1-[2-fluoro-4-(1H-pyrazol-1-yl)phenyl]-5-methoxy-3-(1-phenyl-1H-pyrazol-5-yl)pyridazin-4(1H)-one] is a potent and highly selective inhibitor of PDE10A [13]. Preclinical and clinical data indicate that TAK-063 is safe and well tolerated in humans [14, 15]. Harada et al. demonstrated that PDE10A occupancy increases in the rat striatum following oral administration of TAK-063 in a dose-dependent manner using non-radiolabeled T-773 as a tracer. [16]. In addition, TAK-063 doses of up to 3 mg/kg (orally administered) did not affect plasma prolactin and glucose levels in rats [17]. TAK-063 was shown to cross the blood–brain barrier [18]. Recent studies demonstrated that TAK-063 dose-dependently increased cAMP and cGMP levels [17, 18].

Although PDE10A has been evaluated as treatment target in models of neurodegenerative diseases, its role in acute ischemic stroke has not yet been uncovered. Here, we investigated the neuroprotective effects of PDE10A inhibition by TAK-063 after transient focal cerebral ischemia in mice. To this end, low-dose (0.3 mg/kg) or high-dose (3 mg/kg) TAK-063 were orally administered immediately after ischemia–reperfusion injury induced by intraluminal middle cerebral artery occlusion (MCAO). Neurological deficits, infarct volume, brain swelling, blood–brain barrier (BBB) integrity, disseminated neuronal injury were analyzed by histochemistry, as was cerebral microcirculation, an important denominator of stroke outcome, in the ischemic core and periphery by Laser Speckle Imaging (LSI). Signal pathways and protein responses were evaluated by western blotting, liquid chromatography-tandem mass spectrometry (LC–MS/MS), and planar surface immunoassay.

Materials and Methods

Ethics Statement

Experiments were performed in accordance to the National Institutes of Health (NIH) guidelines for the care and use of laboratory animals and approved by local government authorities (Istanbul Medipol University, Animal Research Ethics Committee). All animals were maintained under a constant 12-h light/dark cycle (lights on at 07:00 daily). Investigators were blinded for experimental groups at all stages of experiments and data analysis.

Experimental Design and Groups

The PDE10A inhibitor TAK-063 was purchased from MedKoo Biosciences (510,331, NC, USA) and suspended in a 1% (v/v) solution of dimethyl sulfoxide (DMSO) in tap water. Adult male C57BL/6j mice weighing 21–26 g was randomly assigned to one of three groups and administered with oral delivery of (i) vehicle (100 µl water containing 1% DMSO), (ii) 0.3 mg/kg TAK-063 (dissolved in 100 µl water containing 1% DMSO), or (iii) 3 mg/kg TAK-063 (dissolved in 100 µl water containing 1% DMSO) at the reperfusion onset. In the first set, vehicle, low dose or high dose of TAK-063 was orally administered without any injury induction ($n = 4$/ group). One hour after oral application of PDE10A inhibitor or vehicle, western blotting analysis was carried out to assess the efficiency of PDE10A inhibition. In the second set, mice were subjected to 90 min of MCAO followed by 24-h reperfusion for the evaluation of neurological score, brain infarct volume, cerebral edema, and serum IgG extravasation ($n = 7$–8 per group). The third set of mice was subjected to 90 min of MCAO followed by 24-h reperfusion for the analysis of cerebral microcirculation by LSI ($n = 4$–5 per group). The fourth set of mice was subjected to 30 min of MCAO and 72-h reperfusion for the analysis of disseminate neuronal injury in the striatum, cytokine/chemokine expression profiles, intracellular signal pathway analysis, and proteomic analysis ($n = 7$–8 per group).

Middle Cerebral Artery Occlusion (MCAO)

Mice were anesthetized with 1% isoflurane (30% O_2, reminder N_2O), and rectal temperature was controlled between 36.5 and 37.0 °C using a feedback-controlled heating system. During the experiments, cerebral blood flow (CBF) was monitored via laser Doppler flowmetry (LDF) using a flexible 0.5 mm fiber optic probe (Perimed, Sweden)

which was attached with tissue adhesive to the intact skull overlying the MCA territory (2 mm posterior and 6 mm lateral from the bregma). Focal cerebral ischemia was induced using an intraluminal filament technique [11]. Briefly, after a midline neck incision, the left common and external carotid arteries were isolated and ligated. A microvascular clip (FE691; Aesculap, Tuttlingen, Germany) was temporarily placed on the internal carotid artery. A 7–0 silicon-coated nylon monofilament (701934PK5Re, Doccol, MA, USA) was inserted through a small incision into the common carotid artery and advanced 9 mm distal to the carotid bifurcation for MCAO. Reperfusion was initiated 30 or 90 min after onset of ischemia by gentle monofilament removal. Thereafter, mice were placed back into their home cages.

In mice subjected to 90-min MCAO, neurological deficits were evaluated 24 h after MCAO using the following 5-point scoring: 0 = normal function, 1 = flexion of torso and of the contralateral forelimb upon lifting of the animal by the tail, 2 = circling to the contralateral side but normal posture at rest, 3 = reclination to the contralateral side at rest, and 4 = absence of spontaneous motor activity. At 72 h (for 30-min MCAO) or 24 h (for 90-min MCAO) after reperfusion, mice were sacrificed under deep anesthesia (4% isoflurane with 30% O_2, remainder N_2O). Brains were removed, frozen on dry ice, and cut on a cryostat into coronal 18-µm sections, which were subsequently used for the analysis of disseminate neuronal injury, infarct volume and brain swelling, and serum IgG extravasation. For 30-min MCAO, tissue samples obtained from the ipsilateral to the stroke were pooled for Western blots.

Analysis of Infarct Volume and Brain Swelling

For the evaluation of infarct volume and brain swelling, coronal brain sections were collected at four equidistant brain levels, 2 mm apart, from mice subjected to 90-min MCAO, which were stained with cresyl violet according to a standard protocol [19]. Within the sections, the border between infarcted and non-infarcted tissues was outlined using an image analysis system (Image J; National Institute of Health, Maryland, USA), and the infarct area was assessed by subtracting the area of the non-infarcted ipsilateral hemisphere from that of the contralateral side. Infarct volume was calculated by integration of these infarct areas. Edema was calculated as the volume difference between the ischemic and the non-ischemic hemisphere and expressed as mm^3.

Analysis of Serum IgG Extravasation

With gentle stirring, brain sections from the bregma 0.0 mm level of mice subjected to 90 min MCAO followed by 24-h reperfusion were rinsed for 10 min at room temperature in 0.1 M phosphate buffered saline (PBS) to remove intravascular IgG and were fixed in 4% paraformaldehyde (PFA) [7]. Following the blocking of endogenous peroxidase with methanol/0.3% H_2O_2 and immersion in 0.1 M PBS containing 5% bovine serum albumin (BSA) and normal swine serum (1:1000), sections were incubated for 1 h in biotinylated horse anti-mouse IgG (BA-1300–2.2, Vectastain Elite; Vector Labs, California, USA) and stained with an avidin peroxidase kit (PK-7800; Vectastain Elite; Vector Labs) and DAB Substrate Kit (SK-4100; Vector Labs). For reasons of data comparability, all sections were processed in parallel. Sections were scanned, and the integrated density of ipsilesional and contralesional hemisphere was quantified using he NIH ImageJ software. Afterward, density of ipsilesional tissue was compared to contralesional tissue to determine BBB leakage. [19].

Laser Speckle Imaging (LSI)

To analyze the effect of low and high dose of TAK-063 on cerebral microcirculation, LSI was performed as described previously [19, 20]. C57BL/6 mice were anesthetized with 1% isoflurane (30% O2, remainder N_2O) and placed in a stereotaxic frame (Stoelting, IL, USA). Throughout the experimental procedure, rectal temperature was maintained between 36.5 and 37.0 °C using a feedback-controlled heating system. A midline incision was made in the scalp, and the skull surface was cleaned with sterile normal saline. Then, mice were subjected to 90-min MCAO as described above followed by the oral delivery of vehicle, low-dose TAK-063 or high-dose TAK-063 at the onset of reperfusion. Cerebral microcirculation was recorded 5 min before the onset of ischemia, during MCAO operations and 90 min after the onset of reperfusion by Pericam PSI System (Perimed). Raw speckle images were taken at 2-s intervals with a spatial image resolution of 20 µm. To analyze CBF changes in the ischemic core and periphery, regions of interest (ROI) covering 1.0 mm × 5.5 mm (in lateral and rostrocaudal direction, respectively) were defined 1.5 and 2.5 mm lateral and 0.5 mm posterior to the bregma, in which mean CBF was calculated using a blood perfusion imaging software (PIMSoft; Perimed) [19]. For each group, CBF changes were given as percent of their own baseline value.

Analysis of Neuronal Survival

Neuronal survival was evaluated as previously described [21]. Coronal brain sections were fixed in 4% PFA/0.1 M PBS, washed, and immersed for 1 h in 0.1 M PBS containing 0.3% Triton X-100 (PBS-T)/10% normal goat serum. Sections were incubated overnight at 4 ºC with Cy3-conjugated monoclonal mouse anti-NeuN (MAB377C3; Merck, NJ, USA). The next day, sections were incubated with 4′,6-diamidino-2-phenylindole (DAPI). Sections were

analyzed using a confocal laser scanning Zeiss LSM 780 microscope (Carl Zeiss, Jena, Germany). Nine different ROI in the striatum, each measuring 62,500 μm^2, were evaluated. Mean numbers of NeuN cells were calculated in the ischemic and contralesional striatum. By dividing the results obtained from ischemic striatum by the results of non-ischemic striatum and multiplying by 100, the percentage of surviving neurons in the ischemic striatum was determined.

Analysis of Neuronal Injury

For the evaluation of DNA fragmentation, coronal brain sections at the level of the striatum from mice subjected to 30 min MCAO were fixed with 4% PFA/0.1 M PBS and were labeled using a TUNEL assay kit (In Situ Cell Death Detection Kit; Roche, Switzerland). Sections were counterstained with 4′,6-diamidino-2-phenylindole (DAPI) [21]. Stainings were analyzed by quantifying TUNEL (+) cells (which in 30-min MCAO are equivalent to neurons) in twelve adjacent ROI in the striatum, each measuring 62,500 μm^2, under a confocal laser scanning Zeiss LSM 780 microscope (Carl Zeiss).

Western Blot

For Western blot analysis, tissue samples harvested from the ischemic striatum belonging to the same group were pooled and homogenized with cell lysis buffer (9803; Cell Signaling Technology, MA, USA) containing protease and phosphatase inhibitor cocktail (5872, Cell Signaling Technology). Proteins were extracted after 15-min centrifugation at 14,000 rpm. Total protein content was evaluated using Qubit 3.0 Fluorometer (Q33216, Invitrogen, Life Technologies Corporation, CA, USA) according to the manufacturer's protocol. Equal amounts of protein (20 μg) were size-fractionated using 4–20% Mini-PROTEAN TGX (4,561,096, Bio-Rad, Life Sciences Research, CA, USA) gel electrophoresis and then transferred to a PVDF membrane using the Trans-Blot Turbo Transfer System (1,704,155, Bio-Rad, Life Sciences Research). Thereafter, membranes were blocked in 5% nonfat milk in 50 mMol Tris-buffered saline (TBS) containing 0.1% Tween (TBS-T; blocking solution) for 1 h at room temperature, washed in 50 mMol TBS-T, and incubated overnight with monoclonal mouse PDE10A (sc-515023; Santa Cruz Biotechnology), polyclonal rabbit anti-phospho-Akt (9275, Cell Signaling Technology), monoclonal rabbit anti-phospho-p44/42 MAPK (Erk1/2) (4370; Cell Signaling Technology), polyclonal rabbit anti-phospho-PTEN (9551; Cell Signaling Technology), polyclonal rabbit anti-phospho-GSK-3α/β (9331; Cell Signaling Technology), polyclonal rabbit anti-phospho-mTOR (2971, Cell Signaling Technology), polyclonal rabbit anti-MMP-9 (Ab38898, Abcam, Cambridge, UK), monoclonal rabbit anti-HIF-1α (36,169; Cell Signaling Technology), polyclonal rabbit anti-Bax (2772; Cell Signaling Technology), or monoclonal rabbit anti-Bcl-xL (2764; Cell Signaling Technology) antibody. On the next day, membranes were washed with 50 mM TBS-T and incubated with horseradish peroxidase-conjugated goat-anti-rabbit (sc-2004; Santa Cruz Biotechnology, Heidelberg, Germany) or goat anti-mouse (sc-2005; Santa Cruz Biotechnology) antibody (diluted 1:2500) for 1 h at room temperature. Blots were performed at least three times. Protein loading was controlled by stripping and re-probing with polyclonal rabbit anti-β-actin antibody (4967, Cell Signaling Technology). Blots were developed using Clarity Western ECL Substrate kit (1,705,060, Bio-Rad; Life Sciences Research) and visualized using the ChemiDoc MP System (1,708,280, Bio-Rad; Life Sciences Research). Intensity of each signal was measured on a total of three digitized blots each using an image analysis system (Image J; National Institute of Health). Protein levels were analyzed densitometrically and corrected with values determined on β-actin blots. The results represented the average of three independent experiments.

Cytokine Array

Tissue sections of the ipsilesional striatum were harvested, homogenized, sonicated, and treated with protease/phosphatase inhibitor cocktail (5872, Cell Signaling Technology). The expression of cytokines was analyzed by the Proteome Profiler Mouse Cytokine Array Panel A Kit (ARY006, R&D Systems, Boston, USA) from a total of 9 animals ($n = 3$ for vehicle, $n = 3$ for 0.3 mg/kg TAK-063, and $n = 3$ for 3 mg/kg TAK-063), according to the manufacturer's recommendation. Array panels were visualized using the ChemiDoc MP System (1,708,280, Bio-Rad). Protein levels were analyzed densitometrically using an image analysis system (Image J), corrected with values determined on positive controls and expressed as relative values compared with vehicle-treated group.

Sample Preparation for Liquid Chromatography Tandem-Mass Spectrometry (LC–MS/MS)

Seventy-two hours after the onset of reperfusion, animals were sacrificed ($n = 4$–5 per group). Thereafter, brains were immediately removed, frozen on dry ice, and stored at − 80 °C. The brain tissues were taken from ipsilesional striatum and were homogenized in 50 mM ammonium bicarbonate and lysed by heating at 95 °C in protein extraction reagent kit (UPX Universal; Expedon, Heidelberg, Germany). Samples were incubated for an hour at 4 °C. After incubation step, samples were centrifuged at 14,000 G for 10 min. Then, supernatants were collected. Protein concentrations were determined via Qubit 3.0 Fluorometer

(Q33216, Invitrogen, Life Technologies) according to the manufacturer's protocol. FASP (Filter Aided Sample Preparation) Protein Digestion Kit (ab270519, Abcam) was used for generating tryptic peptides according to the manufacturer's protocol [22]. A total of 50 µg protein samples were filtered using 6 M urea in a 30-kDa cutoff spin column. After this step, samples were alkylated with 10 mM iodooacetamide in the dark for 20 min at room temperature. Then, samples were incubated overnight with MS grade trypsin protease (ratio 1:100, 90,057, Thermo Scientific) at 37 °C. The following day, peptides were eluted from the columns and lyophilized. At the end of the lyophilization process, the peptides were suspended in 0.1% formic acid (1,002,642,510, Merck) and diluted to 100 ng/µl before injecting to the LC–MS/MS system (ACQUITY UPLC M-Class coupled to a SYNAPT G2-Si high-definition mass spectrometer (Waters, MA, USA)).

LC–MS/MS Analysis and Data Processing

LC–MS/MS and protein identification were performed with small modifications according to previously published protocols [23, 24]. The samples were loaded onto the ACQUITY UPLC M-Class coupled to a SYNAPT G2-Si high-definition mass spectrometer (Waters). To equilibrate the columns, 97% of mobile phase (including 0.1% formic acid in UHPLC grade water) was used, and column was heated to 55 °C. Ninety-minute gradient elution from the trap column ACQUITY UPLC M-Class Symmetry C18 trap column (180 µm × 20 mm; 186,007,496, Waters) to the analytic column (ACQUITY UPLC M-Class HSS T3 Column, 100 Å, 1.8 µm, 75 µm × 250 mm; 186,007,474, Waters) at 0.400 µl/min flow rate with a gradient from 4 to 40% hypergrade acetonitrile (100,029, Merck) containing 0.1% formic acid (v/v) was used for the peptide separation. Positive ion modes of MS and MS/MS scans with 0.7-s cycle time were performed sequentially. Ten volts was set as low collision energy and 30 V as high CE. Ion mobility separation (IMS) was used for the ion separation. A wave velocity was ramped from 1000 to 55 m/s over the full IMS cycle. The release time for mobility trapping was set as 500 µs, and trap height was set to 15 V. IMS wave delay was 1000 µs for the mobility separation after trap release [25]. Without any precursor ion preselection, all the ions within 50–1900 m/z range were fragmented in resolution mode. Additionally, 100 fmol/µl Glu-1-fibrinopeptide B was infused as lockmass reference with a 60-s interval. Progenesis-QI for proteomics software (Waters) was used for the identification and quantification of the peptides. Whole proteins were identified by at least 2 unique peptide sequences, and then, the expression ratio of proteins was calculated.

Statistical Analysis

Statistical analysis was performed using SPSS (version 15, SPSS Inc., Chicago USA) software. Data were evaluated by one-way ANOVA followed by LSD tests. Data are presented as mean ± S.D. values. Throughout the study, p values < 0.05 were considered as statistically significant.

Results

Low-dose (0.3 mg/kg) and high-dose (3 mg/kg) TAK-063 reduced striatal PDE10A protein abundance

Both low (0.3 mg/kg) and high (3 mg/kg) doses of orally administered TAK-063 reduced PDE10A protein abundance in the mouse striatum within 1 h (Fig. 1a), providing evidence that PDE10A was efficiently blocked by the inhibitor. PDE10A protein level was reduced to 75 ± 13.7 and 48.8 ± 3.6 respectively, in mice receiving 0.3 mg/kg and 3 mg/kg TAK-063, as compared to vehicle-treated mice.

Effects of TAK-063 on Neurological Deficit Score, Infarct Size, Cerebral Edema, and Blood–Brain Barrier Permeability

To ensure reproducible brain injury among the experimental groups, cerebral blood flow (CBF) was monitored and analyzed in real time via laser Doppler flow (LDF) measurement using a flexible probe attached to the animals' skulls above the core of the MCA region (Figs. 1b and 3a). We noted that TAK-063 doses used in this study resulted in a slightly higher CBF during reperfusion compared to the control group animals; however, this increase was not significant. Twenty-four hours after 90-min ischemia, four-point neurological scoring was performed for the evaluation of neurological deficits. Infarct volume and brain edema were evaluated by cresyl violet staining. In this model of combined subcortical-cortical infarction, low and high-dose TAK-063 significantly reduced stroke-related neurological deficits, infarct volume, and brain edema (Fig. 1c–e). Besides, BBB permeability assessed by serum IgG extravasation was decreased by low-dose, but not high-dose TAK-063 (Fig. 1f).

PDE10A Inhibition Increases Regional Microcirculation in Ischemic Core Region

To analyze the hemodynamic effects induced by orally administered TAK-063, we further evaluated regional cerebral microcirculation in the ischemic core (Fig. 2b) and ischemic periphery (Fig. 2c) by Laser Speckle Imaging (LSI). For this aim, mice were subjected to 90-min

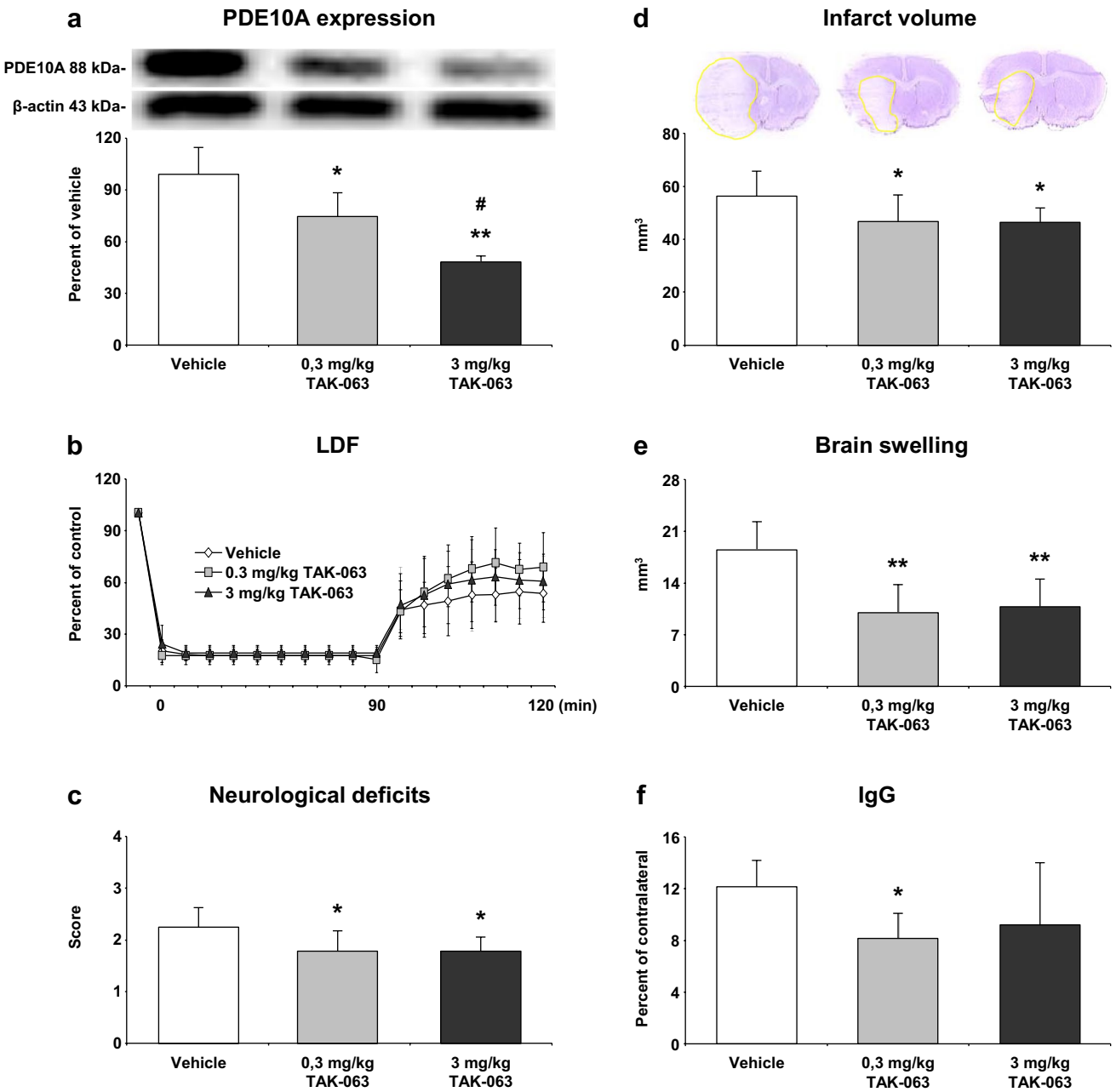

Fig. 1 Effects of PDE10A inhibition by TAK-063 on PDE10A expression, neurological deficits, infarct volume, brain swelling, and blood–brain barrier leakage. Both low (0.3 mg/kg) and high (3 mg/kg) doses of TAK-063 significantly reduced PDE10A protein expression in the striatum (**a**). Western blots are representative of three independent experiments. Cerebral blood flow (CBF) was analyzed via laser Doppler flowmetry (LDF) during MCAO experiments (**b**). In addition, low dose or high dose of TAK-063 decreased neurological deficits (**c**), infarct volume (**d**), and brain swelling (**e**). Only low of dose of TAK-063 significantly reduced blood–brain barrier (BBB) permeability (**f**) evaluated by serum IgG extravasation in mice submitted to 90 min of intraluminal MCAO, which induces brain infarcts of the striatum and overlying cortex. Data are represented as mean + S.D. ($n = 7$–8 mice/group). $^{**}p < 0.01$/$^{*}p < 0.05$ compared with vehicle, $^{\#}p < 0.05$ compared with 0.3 mg/kg TAK-063-treated group

MCAO which is followed by secondary hypoperfusion that develops within 90 min after reperfusion onset [26]. Low-dose TAK-063 which was administered at the beginning of the reperfusion significantly increased regional microcirculation in the ischemic core region starting 30 min after reperfusion onset, while high-dose TAK-063 increased microcirculation in a more delayed fashion starting 100 min after reperfusion onset. Effects of TAK-063 on

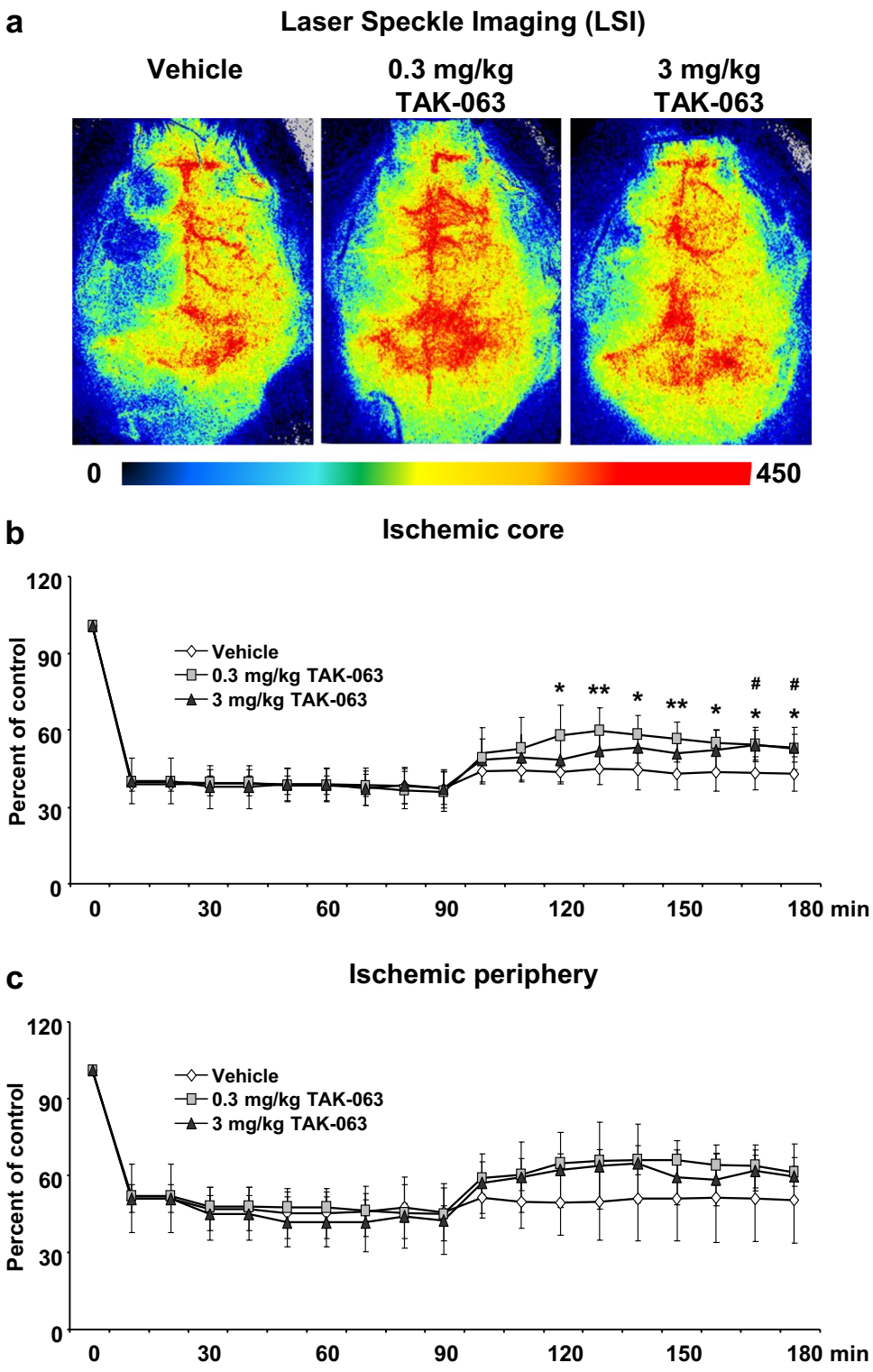

Fig. 2 Effects of TAK-063-mediated PDE10A inhibition on post-ischemic regional cerebral blood flow. Representative images of Laser Speckle Imaging (LSI) (**a**), and semi-quantitative analysis of regional CBF in the ischemic core (**b**) and in the ischemic periphery (**c**) evaluated by LSI in mice subjected to 90 min of intraluminal MCAO. Low dose (0.3 mg/kg) or high dose (3 mg/kg) of TAK-063 was orally administered immediately following the onset of reperfusion. Twenty minutes after the onset of reperfusion, 0.3 mg/kg TAK-063 significantly increased regional cerebral microcirculation in the ischemic core territory. Besides this, 3 mg/kg TAK-063 increased cerebral microcirculation in the ischemic core area 70 min after the onset of reperfusion. Although CBF in the ischemic periphery was slightly affected, no statistical difference was observed. Data are represented as mean + S.D. ($n = 4$–5 mice/group). $^{**}p < 0.01$/$^{*}p < 0.05$ shows significant differences between vehicle and 0.3 mg/kg TAK-063 group, $^{\#}p < 0.05$ shows significant differences between vehicle and 3 mg/kg TAK-063 group

cerebral microcirculation in the ischemic periphery did not achieve significance. Hence, the microcirculatory effects of low-dose TAK-063 were more pronounced than those of high-dose TAK-063.

Effect of PDE10A Inhibition on Disseminate Neuronal Injury

We next examined the effects of PDE10A inhibition in a model of mild focal cerebral ischemia induced by 30-min

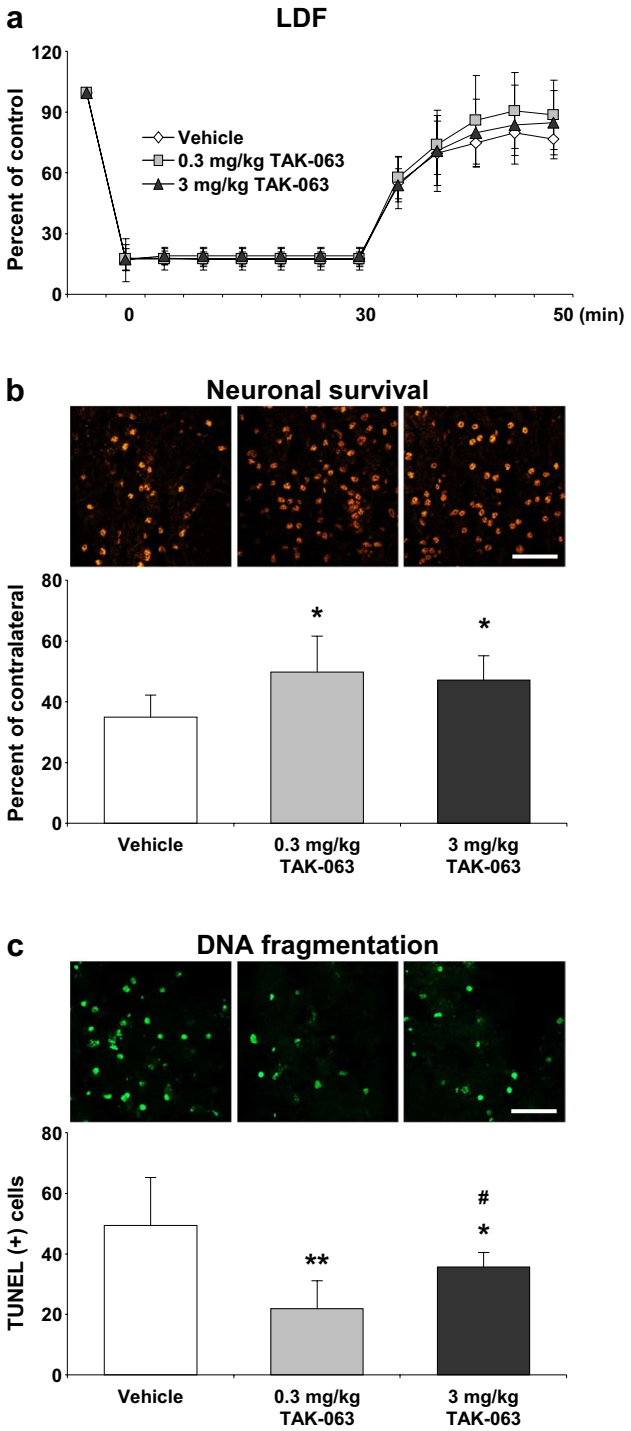

Fig. 3 TAK-063 increased neuronal survival and decreased disseminated neuronal injury after cerebral ischemia. CBF (**a**) was controlled via LDF during ischemia and at the onset of reperfusion. The low dose (0.3 mg/kg) and high dose (3 mg/kg TAK-063) of TAK-063 increased neuronal survival (**b**) after transient focal cerebral ischemia. In addition, both low and high dose of TAK-063 decreased the number of apoptotic cells (**c**) in the ischemic striatum. Data are represented as mean + S.D. ($n = 7$–8 mice/group). $^{**}p < 0.01$/$^{*}p < 0.05$ compared with vehicle, $^{\#}p < 0.05$ compared with 0.3 mg/kg TAK-063-treated group. Scale bars are 50 µm (**b**–**c**)

MCAO, which induces disseminate neuronal injury in the striatum developing over 1 to 3 days [27]. In this model, low-dose and high-dose TAK-063 increased neuronal survival and decreased the number of DNA-fragmented (that is, irreversibly injured) cells in the ischemic striatum (Fig. 3b–c). Hence, PDE10A inhibition efficiently provided protection against a wide range of ischemic injury severities, preventing combined subcortical-cortical infarction and disseminate neuronal death at the same time.

PDE10A Inhibition with TAK-063 Regulates Survival-Related Proteins

Western blot analysis was used to evaluate the effect of PDE10A inhibition with TAK-063 on cellular survival and apoptosis-related protein levels in the ischemic striatum. Seventy-two hours after 30-min MCAO, PDE10A protein abundance was still reduced in the ischemic striatum (Fig. 4a). Both doses of TAK-063 increased the level of phosphorylated (that is, activated) Akt (Thr308) (Fig. 4b) and phosphorylated (that is, activated) GSK3 α/β (Fig. 4c) and decreased the level of phosphorylated (that is, inactive) mTOR (mammalian target of rapamycin) (Fig. 4d). Low-dose TAK-063 also significantly increased the level of phosphorylated (that is, activated) ERK-1/2 (Fig. 4e) and decreased the level of phosphorylated (that is, inactive) PTEN (Fig. 4f). These data indicated that TAK-063 elicited a robust response of pro-survival proteins that contributed to post-ischemic neuroprotection induced by PDE10A inhibition.

In line with the stabilization of post-ischemic reperfusion and the stabilization of BBB integrity, the abundance of hypoxia inducible factor-1α (HIF-1α) (Fig. 4g) and matrix metalloproteinase-9 (MMP-9) (Fig. 4h) were significantly decreased by TAK-063. Moreover, we also evaluated the expression of pro-apoptotic Bax and anti-apoptotic Bcl-xL in the ipsilesional striatum. Both doses of TAK-063 significantly decreased Bax protein abundance and increased anti-apoptotic Bcl-xL protein abundance (Fig. 4i–j).

TAK-063 Altered the Cytokine/Chemokine Expression Profile After Focal Cerebral Ischemia

The stabilization of BBB integrity by TAK-063 subsequently prompted us to evaluate the levels of cytokines and chemokines in the ischemic brain. The relative expression levels of 40 different cytokines and chemokines (CXCL13/BLC/BCA-1, C5a, G-CSF, GM-CSF, CCL1/I-309, CCL11/Eotaxin, ICAM-1, IFN-gamma, IL-1 alpha/IL-1F1, IL-1 beta/IL-1F2, IL-1ra/IL-1F3, IL-2, IL-3, IL-4, IL-5, IL-6, IL-7, IL-10, IL-12 p70, IL-13, IL-16, IL-17, IL-23, IL-27, CXCL10/IP-10, CXCL11/I-TAC, CXCL1/KC, M-CSF, CCL2/JE/MCP-1, CCL12/MCP-5, CXCL9/MIG, CCL3/

MIP-1 alpha, CCL4/MIP-1 beta, CXCL2/MIP-2, CCL5/RANTES, CXCL12/SDF-1, CCL17/TARC, TIMP-1, TNF-alpha, and TREM-1) in the ipsilesional striatum were evaluated using an antibody array (Fig. 5a). These analyses revealed a broad anti-inflammatory response. As such, the expression of G-CSF, I-309, INF-γ, IL-1α, IL-1β, IL-1ra, IL-2, IL-3, IL-7, IL-13, IL-16, IL-17, IL-23, IL-27, IP-10, I-TAC, KC, M-CSF, JE, MCP-5, MIG, MIP-1α, MIP-1β, MIP-2, RANTES, TNF-α, and TREM-1 was decreased by TAK-063 (Fig. 5b). BLC, C5/C5a, IL-4, SDF-1, TARC, and TIMP-1 were not influenced by TAK-063 (Fig. 5b).

TAK-063-Mediated PDE10A Inhibition Altered Protein Profile in the Ipsilesional Striatum

To understand the changes in the protein profile after TAK-063 administration, ischemic tissues were analyzed by liquid chromatography-tandem mass spectrometry (LC–MS/MS). A total of 1721 proteins were identified in vehicle and TAK-063-treated groups. Forty different proteins were significantly altered by low-dose/high-dose TAK-063 treatment (Fig. 6). These proteins are 26S proteasome non-ATPase regulatory subunit 2 (PSMD2), 40S ribosomal protein S18 (RPS18-PS5), acyl-CoA thioesterase 7 (ACOT7), ADP/ATP translocase 1 (ADT1), ankyrin repeat and sterile alpha motif domain-containing protein 1B (ANKS1B), centromere-associated protein E (CENPE), cytoplasmic FMR1-interacting protein 1 (CYFP1), dedicator of cytokinesis protein 4 (DOCK4), dihydrolipoyl dehydrogenase, mitochondrial (DLDH), DNA polymerase epsilon catalytic subunit A (DPOE1), DNA polymerase zeta catalytic subunit (REV3L), dynactin subunit 4 (DCTN4), electron transfer flavoprotein subunit beta (ETFB), extracellular matrix protein 2 (ECM2), filamin-A (FLNA), flotillin (FLOT2), hydroxyacylglutathione hydrolase, mitochondrial (HAGH), importin subunit alpha-4 (IMA4), LanC-like protein 2 (LANCL2), long-chain-fatty-acid–CoA ligase ACSBG1 (ACBG1), microtubule-associated protein RP/EB family member 2 (MAPRE2), NADH-ubiquinone oxidoreductase 18 kDa subunit (NDUFS4), ornithine aminotransferase, mitochondrial (OAT), phosphatidylinositol 4-phosphate 5-kinase type-1 gamma (PIP5K1C), phosphofurin acidic cluster sorting protein 1 (PACS1), proteasome subunit beta type-1 (PSMB1), protein S100-B (S100B), pyridoxal phosphate homeostasis protein (PLPHP), Ras-related protein Rab-8B (RAB8B), Rho GTPase-activating protein 23 (ARHGAP23), Rho-associated protein kinase 2 (ROCK2), secretory carrier-associated membrane protein (SCAMP1), serpin B6 (SERPINB6), sodium leak channel non-selective protein (NALCN), solute carrier family 25 member 11 (SLC25A11), solute carrier family 25 member 12 (SLC25A12), T-complex protein 1 subunit epsilon (TCPE), tyrosine-protein phosphatase non-receptor type substrate 1 (SHPS1), tyrosine–tRNA ligase, cytoplasmic (SYYC), voltage-dependent anion-selective channel protein 3 (VDAC3).

Identified proteins were clustered into groups based on their molecular function and biological process using the PANTHER (protein annotation through evolutionary relationship) classification system (http://www.pantherdb.org/). Molecular function classification included proteins with binding, catalytic, and transporter activity. PANTHER classification based on biological process included five predominant groups: cellular process, metabolic process, localization, biological regulation, and response to stimulus. In addition to this, six signaling pathways were identified as cytoskeletal regulation by Rho GTPase, dopamine receptor-mediated signaling pathway, Huntington's disease, integrin signaling pathway, Parkinson's disease, and ubiquitin proteasome pathway.

Discussion

Phosphodiesterases (PDEs) are subdivided into 11 families and encoded by 21 genes resulting in more than 100 functionally distinct enzymes produced by alternative splicing [28, 29]. Among them, the dual substrate enzyme PDE10A, which is highly abundant in the mammalian striatum, acts as an essential cell signaling regulator which acts by hydrolyzing the second messengers, cGMP and cAMP [1, 2]. Therefore, it is suggested that PDE10A may play an essential role in the modulation of striatal neuronal activity in motor and cognitive processes [6, 12, 30]. Recent studies suggested that PDE10A can be an important target, especially in neurodegenerative diseases due to its modulatory roles in the CNS. To this end, we investigated the role of PDE10A in ischemic injury development.

To our knowledge, this is the first study showing the neuroprotective effects of PDE10A inhibition in an ischemic stroke model. We therefore investigated molecular pathways mediating neuroprotection. PDE10A was effectively blocked by the PDE10A inhibitor, as shown by the fact that TAK-063 dose-dependently reduced striatal PDE10A abundance. Inhibition of PDE10A causes an increase in cAMP and cGMP levels which are responsible for activation of PKA and cGMP-dependent protein kinase (PKG). Activated PKA and PKG increase the phosphorylation state of cAMP response element-binding protein (CREB) and alpha-amino-3-hydroxy-5-methylisoxazole-4-propionic acid (AMPA)-type glutamate receptors [17].

PDE10A enzyme has a C-terminal catalytic domain and N-terminal tandem GAF domains that cAMP can bind and stimulate its activity [18]. In addition, cAMP-dependent phosphorylation of PDE10A by PKA was reported [17]. In human studies with PDE10A mutations, it was shown that

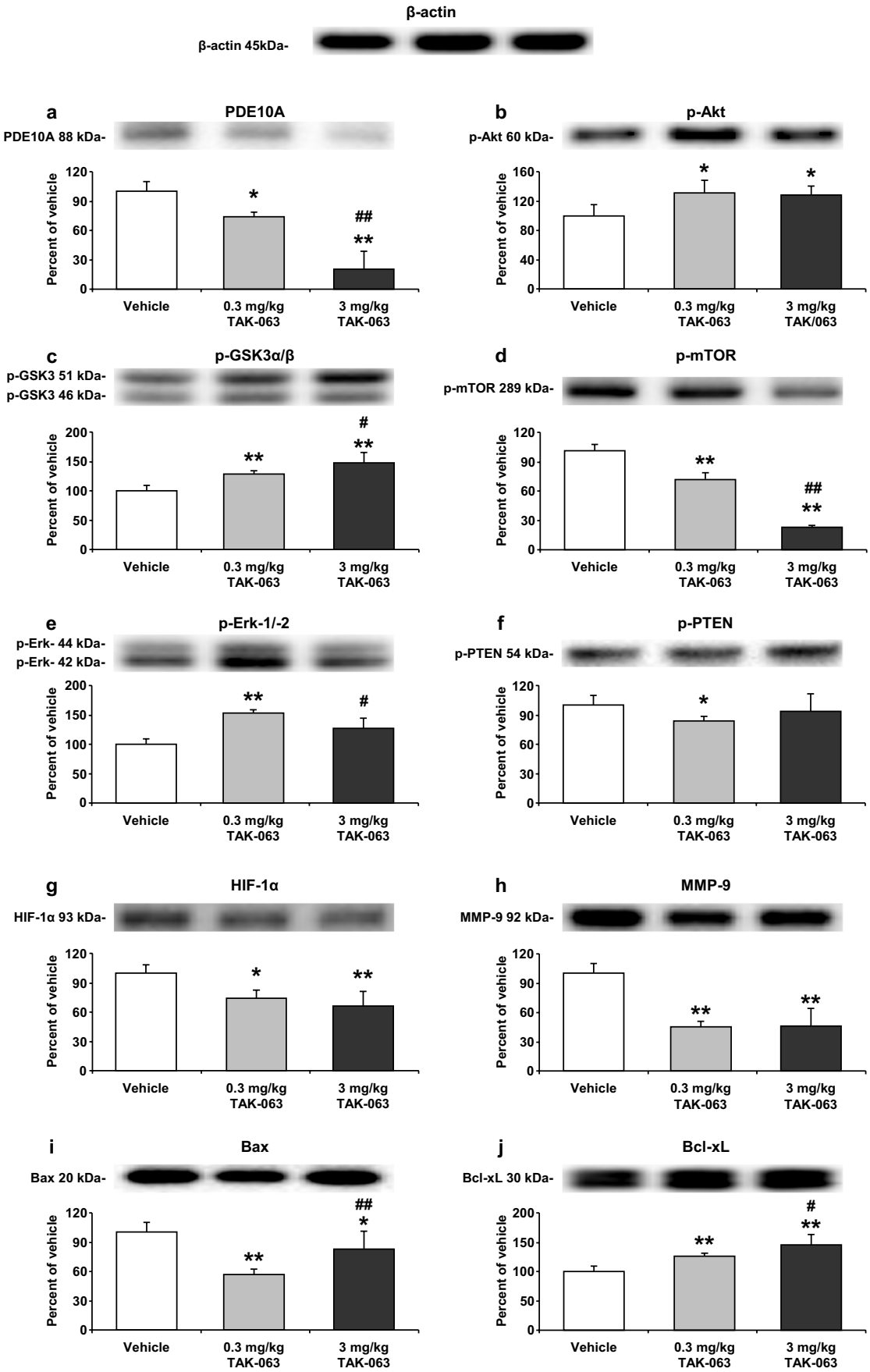
β-actin
β-actin 45kDa-
a
PDE10A
PDE10A 88 kDa-
Percent of vehicle
Vehicle
0.3 mg/kg TAK-063
3 mg/kg TAK-063
b
p-Akt
p-Akt 60 kDa-
3 mg/kg TAK/063
c
p-GSK3α/β
p-GSK3 51 kDa-
p-GSK3 46 kDa-
d
p-mTOR
p-mTOR 289 kDa-
e
p-Erk-1/-2
p-Erk- 44 kDa-
p-Erk- 42 kDa-
f
p-PTEN
p-PTEN 54 kDa-
g
HIF-1α
HIF-1α 93 kDa-
h
MMP-9
MMP-9 92 kDa-
i
Bax
Bax 20 kDa-
j
Bcl-xL
Bcl-xL 30 kDa-

◂**Fig. 4 TAK-063 re-regulates neuronal survival-related proteins and pro/anti-apoptotic proteins after focal cerebral ischemia.** Western blots for PDE10A (**a**), p-Akt (**b**), p-GSK3 α/β (**c**), p-mTOR (**d**), p-Erk-1/-2 (**e**), p-PTEN (**f**), HIF-1α (**g**), MMP-9 (**h**), Bax (**i**), and Bcl-xL (**j**) in the ischemic tissue samples obtained from brains of mice submitted to 30 min of intraluminal MCAO followed by 72-h reperfusion. Note that the level of survival kinase p-Akt, p-GSK3 α/β, and anti-apoptotic Bcl-xL protein was significantly increased and PDE10A, p-mTOR, HIF-1α, MMP-9, and pro-apoptotic Bax protein expression was significantly reduced by TAK-063 treatments. In addition, only low dose of TAK-063 group significantly increased the level of p-Erk-1/-2 and significantly decreased the level of p-PTEN. On top of the figure, a representative β-actin blot is shown. Representative images of Western blot analysis from three independent experiments were given above their corresponding graphs. Data are represented as mean ± S.D. values of three independent experiments. $^{**}p < 0.01/^{*}p < 0.05$ compared with vehicle, $^{\#\#}p < 0.01/^{\#}p < 0.05$ compared with 0.3 mg/kg TAK-063-treated group

several mutations of these domains of PDE10A lead to the reduction of protein levels, possibly through the blockade of PKA phosphorylation and subsequent ubiquitination and degradation of PDE10A [31, 32]. As a result, TAK-063 binding to the catalytic domain may physically block the phosphorylation by PKA, and this may cause the protein to be degraded by proteasomal activity and by autophagy. Moreover, it is well-known that raising cAMP and cGMP levels by PDE inhibitors can stimulate 26S proteasome activity and degradation of several types of proteins. It has been reported that increased cGMP levels by using different PDE5 inhibitors resulted in the stimulation of ubiquitin conjugation and, hence, an increase in the amount of ubiquitinated proteins. In addition to the increased ubiquitinated proteins, enhanced proteasomal function resulted in the degradation of several short-lived or long-lived proteins [33–35]. Therefore, we think it is possible that TAK-063-mediated increased cAMP and cGMP levels are (at least partially) responsible for the proteasomal degradation of PDE10A enzyme levels.

Here, we showed that TAK-063-mediated PDE10A inhibition decreased neurological deficits after focal cerebral ischemia. It is well-established that the MCAO model used in this study causes an infarct size that is directly related to the degree of brain edema and BBB leakage [19, 24, 36]. Therefore, we evaluated infarct volume, brain swelling, and blood–brain barrier (BBB) permeability in mice submitted to 90-min MCAO, which is a model of combined subcortical-cortical infarction, and disseminate neuronal injury in the striatum of mice exposed to 30-min MCAO. To the best of our knowledge, this is the first study demonstrating the neuroprotective efficacy of PDE10A inhibition in ischemic brain injury. Both TAK-063 doses reduced the infarct volume and brain edema after 90-min MCAO. In addition, 0.3 mg/kg TAK-063 increased BBB integrity. After 30-min MCAO, both TAK-063 doses reduced disseminate neuronal injury. That PDE10A inhibition similarly protected against combined subcortical-cortical infarction, and disseminate neuronal injury emphasizes the critical role of PDE10A in ischemic injury development.

Focal cerebral ischemia induced by MCAO dramatically decreases CBF in the ischemic core region. Cessation of glucose and oxygen delivery and depletion of ATP in the ischemic core results rapid necrotic cell death of neurons and glial cells [37, 38]. However, the area surrounding the ischemic core and the ischemic periphery exhibit more moderate CBF reduction allowing neurons to survive for a limited time [37]. In the present study, we first examined CBF by LDF which provides instantaneous and continuous measurements of microcirculation over small area of brain tissue [39, 40]. CBF was slightly but not significantly increased by TAK-063 treatment. To investigate the changes in CBF, the 90-min MCAO model, which appropriately allows the analysis of CBF changes in the cerebral cortex using LSI, was chosen [19, 20]. CBF in the cortex was monitored during MCAO operations and in the first 90 min of reperfusion via LSI which is a more powerful and accurate tool to analyze microcirculation in real time in a large brain region. It should be noted that both TAK-063 treatments increased regional CBF in the ischemic core region, although higher dose induced significantly increased CBF levels later than the lower dose. This delayed increase in blood flow in the higher dose might be due to the accumulation of cAMP/cGMP levels in response to PDE10A inhibition. Further studies are required to undercover the mechanism of effect of TAK-063 in the cerebral blood flow regulation.

To investigate the mechanism underlying TAK-063-induced recovery after focal cerebral ischemia, we analyzed signal transduction pathways which were related to neuronal survival, apoptosis, and cellular energy homeostasis via western blot. To this end, we evaluated ipsilesional tissue samples from mice subjected to 30-min MCAO. It has been reported that this model of cerebral ischemia induces selective neuronal injury in the striatum [19]. In addition to this, PDE10A is almost exclusively expressed in the striatum [12, 30]. We observed that PDE10A protein expression was still reduced in a dose-dependent manner even 72 h after oral administration of TAK-063 in mice. It was observed that low dose of TAK-063 reduced PTEN phosphorylation, which is a negative regulator of phosphatidylinositol-3 kinase (PI3K) and increased Akt phosphorylation after focal cerebral ischemia. It is well known that PI3K/Akt signaling controls neuronal survival, cell proliferation, apoptosis, glucose metabolism, and inflammation [41–43]. Besides, activation of Akt leads to inhibition of apoptosis by phosphorylation of downstream molecules such as glycogen synthase kinase-3 (GSK3) which is active only when dephosphorylated [44]. Our results suggest that TAK-063 increases the phosphorylation status of GSK3 in a dose-dependent manner. Notably, expression of the mammalian target of rapamycin (mTOR), which is an essential regulator of cell metabolism, cell

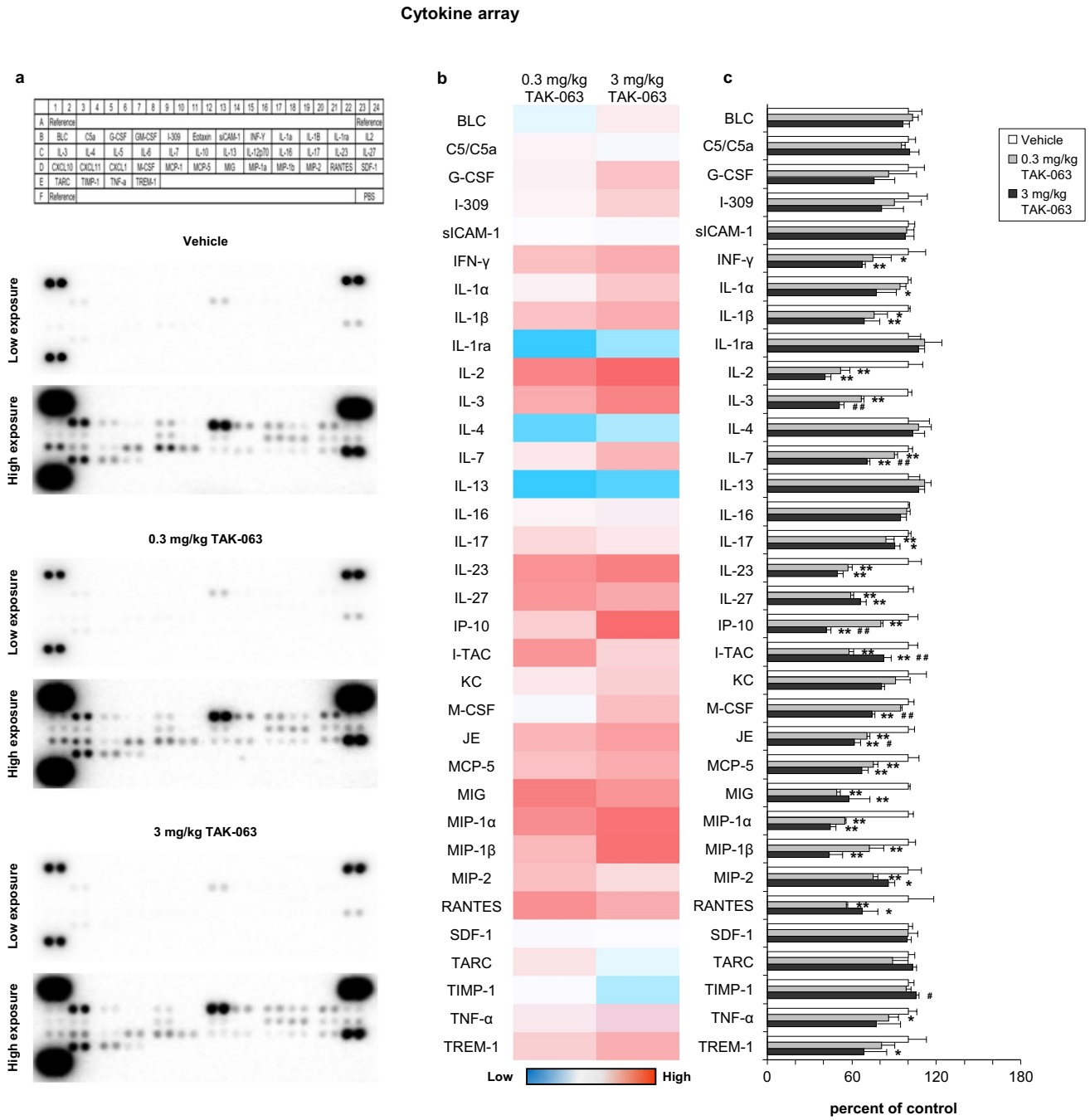

Fig. 5 Heat map and bar graph visualization of the cytokines/chemokine's analysis. Representative images for cytokine array panels (**a**). The cytokine and chemokine levels in the ipsilesional striatum from animals submitted to 30-min MCAO followed by 72-h reperfusion, analyzed by a Proteome Profiler Mouse Cytokine Arrays. Results obtained from cytokine/chemokine arrays are visualized in the heat map (**b**) and in the bar graph (**c**). Data are represented as mean ± S.D. values. $^{**}p < 0.01/^{*}p < 0.05$ compared with vehicle, $^{\#\#}p < 0.01/^{\#}p < 0.05$ compared with 0.3 mg/kg TAK-063-treated group

growth, proliferation, and survival, is decreased in a dose-dependent manner after ischemia [45]. TAK-063 increased phosphorylation of extracellular signal-regulated protein kinases 1 and 2 (ERK1/2) which plays an essential role in as the regulation of cell proliferation and apoptosis.

Accumulating evidence have demonstrated that hypoxia-inducible factor-1α (HIF-1α) which is a hypoxia-responsive gene, plays an essential role after ischemia/reperfusion injury [46–48]. Inhibition of PDE10A significantly decreases HIF-1α protein expression in the ipsilesional

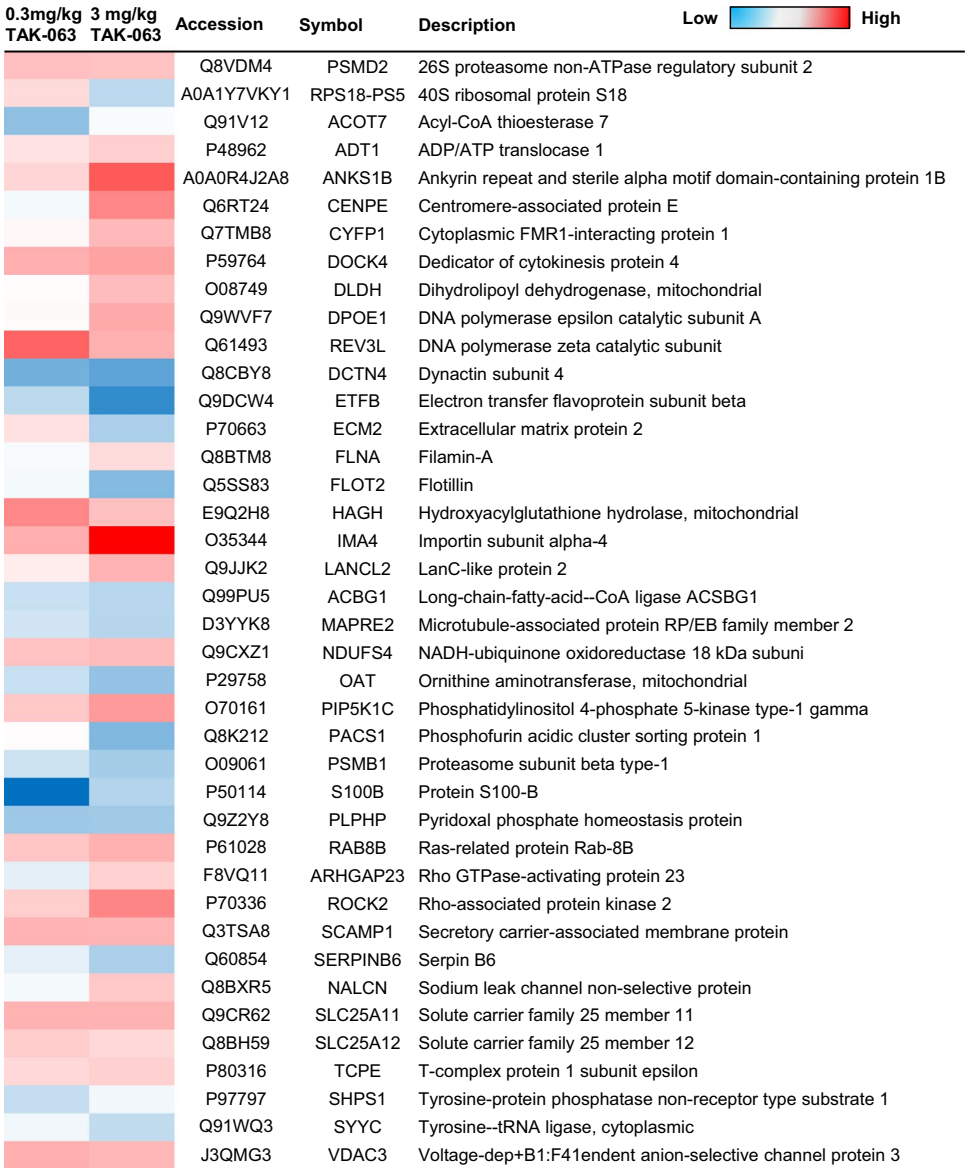

Fig. 6 Identification of TAK-063 related proteins and their regulation after 30 min of intraluminal MCAO via liquid chromatography-tandem mass spectrometry (LC–MS/MS). A total of 40 different proteins were identified between vehicle and low-dose/high dose of TAK-063-mediated PDE10A inhibition groups. Comparisons (0.3 mg/kg TAK-063/vehicle ratio and 3 mg/kg TAK-063/vehicle ratio) of differential protein expression were given by heat map analysis

tissue. Focal cerebral ischemia causes the disruption of BBB which protects the brain from harmful substances, toxins, and inflammation [49]. Furthermore, it is well known that protein expression of matrix metalloproteinases (MMPs), specifically MMP-9 levels, increases after ischemia which is highly related to BBB leakage [50]. The results obtained in this study showed that TAK-063 profoundly diminished MMP9 protein expression after ischemic stroke. Anti-apoptotic Bcl-xL and pro-apoptotic Bcl-2-associated X-protein (Bax) play critical roles in the regulation of signal transduction pathways in apoptosis [51]. Following ischemia, oral delivery of TAK-063, especially low dose, decreased pro-apoptotic Bax protein expression. In addition, anti-apoptotic Bcl-xL protein expression was increased by TAK-063 in a dose-dependent manner after ischemia.

It should be noted that cell death after focal cerebral ischemia triggers the activation of cytokines and chemokine production which contribute to the progression of the ischemic injury. Animal studies and clinical studies demonstrated that increased pro-inflammatory cytokine production and decreased anti-inflammatory cytokine production increase brain damage in experimental models of ischemic stroke [52]. In the present study, we investigated the expression profile of cytokines and chemokines 72 h after 30 min of MCAO. Expression of pro-inflammatory cytokines/chemokines I-309, INF-γ, IL-1α, IL-1β, IL-2, IL-3, IL-7, IL-23, IP-10, KC, JE, MCP-5, MIP-1α, MIP-1β, TNF-α, and TREM-1 was decreased in a dose-dependent manner after ischemia. However, low dose of TAK-063 decreased pro-inflammatory cytokines/chemokines IL-17, I-TAC, MIG, MIP-2, and RANTES protein expression more than high

dose of TAK-063. Moreover, PDE10A inhibition increased expression of anti-inflammatory cytokines/chemokines IL-1ra, IL-4, IL-13, and TIMP-1. Interestingly, expression of G-CSF, IL-27, and M-CSF which are known as anti-inflammatory cytokines/chemokines was decreased. In addition, pro-/anti- inflammatory cytokines/chemokines BLC, C5/C5a, sICAM-1, IL-16, SDF-1, and TARC were not influenced by TAK-063.

LC–MS/MS-based proteomics serve an emerging tool to understanding of the molecular and cellular mechanisms of neurodegenerative disorders including Parkinson's disease, Alzheimer's disease, and cerebral ischemia [24, 53–55]. In the present study, we examined the protein profile changes in the ischemic brain induced by PDE10A inhibition. For this purpose, ipsilesional tissues from mice subjected to 30-min MCAO followed by 72-h reperfusion were analyzed by LC–MS/MS. For the first time, proteins that had significantly been altered by low-dose or high-dose TAK-063 have been identified. PSMD2, ADT1, ANKS1B, CYFP1, DLDH, DPOE1, DOCK4, REV3L, FLNA, HAGH, IMA4, LANCL2, NDUFS4, PIP5K1C, RAB8B, ARHGAP23, ROCK2, SCAMP1, NALCN, SLC25A11, SLC25A12, TCPE, and VDAC3 proteins were increased, and ACOT7, DCTN4, ETFB, FLOT2, ACBG1, MAPRE2, OAT, PACS1, PSMB1, S100B, PLPHP, SERPINB6, SHPS1, and SYYC were decreased by TAK-063 treatments. Clustering of proteins into groups based on their molecular function and biological process using PANTHER (http://www.pantherdb.org/) revealed that the proteins identified included proteins with binding, catalytic, and transporter activity. PANTHER classification based on biological process revealed five predominant groups (cellular process, metabolic process, localization, biological regulation, and response to stimulus). In addition to this, six signaling pathways were identified as cytoskeletal regulation by Rho GTPase, dopamine receptor-mediated signaling pathway, Huntington's disease, integrin signaling pathway, Parkinson's disease, and ubiquitin proteasome pathway, demonstrating a profound effect of PDE10A on neuronal survival-associated cell signaling.

In conclusion, this study indicated that both low dose (0.3 mg/kg) and high dose (3 mg/kg) of TAK-063 reduced neurological deficits, infarct volume, brain swelling, BBB leakage, and neuronal injury in the ischemic brain, which was associated with re-regulation of anti-apoptotic and pro-apoptotic proteins, re-regulation of the PI3K/Akt signal transduction pathway, decreased pro-inflammatory cytokine/chemokine responses, and increased anti- inflammatory cytokine/chemokine responses. Our study identifies PDE10A as a potent target for neuroprotective therapies that in view of the restorative effect of PDE10A inhibition [12] deserves further scrutiny.

Author Contribution This work was carried out in collaboration between all authors. MCB, ABC, and SA carried out experimental work, analyzed data, and helped to write the manuscript. EO and TK performed LC–MS/MS experiments and analyzed data. NA and BC carried out Western blot and immunofluorescence studies. MCB, TRD, UK, DMH, and EK defined the research theme and revised the manuscript critically.

Funding This work was supported by TUBITAK (The Scientific and Technological Research Council of Turkey/ 218S453; MCB) and Turkish Academy of Sciences (TUBA; EK).

Data availability The datasets analyzed during the current study are available from the corresponding author on reasonable request.

Code Availability Not applicable.

Declarations

Ethics Approval Experiments were performed in accordance to National Institutes of Health (NIH) guidelines for the care and use of laboratory animals and approved by local government authorities (Istanbul Medipol University, Animal Research Ethics Committee).

Consent to Participate Not applicable.

Consent for Publication Not applicable.

Conflict of Interest The authors declare no competing interests.

References

1. Fujishige K, Kotera J, Michibata H, Yuasa K, Takebayashi S, Okumura K, Omori K (1999) Cloning and characterization of a novel human phosphodiesterase that hydrolyzes both cAMP and cGMP (PDE10A). J Biol Chem 274(26):18438–18445. https://doi.org/10.1074/jbc.274.26.18438
2. Soderling SH, Bayuga SJ, Beavo JA (1999) Isolation and characterization of a dual-substrate phosphodiesterase gene family: PDE10A. Proc Natl Acad Sci U S A 96(12):7071–7076. https://doi.org/10.1073/pnas.96.12.7071
3. Kelly MP (2018) Cyclic nucleotide signaling changes associated with normal aging and age-related diseases of the brain. Cell Signal 42:281–291. https://doi.org/10.1016/j.cellsig.2017.11.004
4. Cardinale A, Fusco FR (2018) Inhibition of phosphodiesterases as a strategy to achieve neuroprotection in Huntington's disease. CNS Neurosci Ther 24(4):319–328. https://doi.org/10.1111/cns.12834
5. Persson J, Szalisznyo K, Antoni G, Wall A, Fallmar D, Zora H, Boden R (2020) Phosphodiesterase 10A levels are related to striatal function in schizophrenia: a combined positron emission tomography and functional magnetic resonance imaging study. Eur Arch Psychiatry Clin Neurosci 270(4):451–459. https://doi.org/10.1007/s00406-019-01021-0
6. Xie Z, Adamowicz WO, Eldred WD, Jakowski AB, Kleiman RJ, Morton DG, Stephenson DT, Strick CA, Williams RD, Menniti FS (2006) Cellular and subcellular localization of PDE10A, a striatum-enriched phosphodiesterase. Neuroscience 139(2):597–607. https://doi.org/10.1016/j.neuroscience.2005.12.042

7. Seeger TF, Bartlett B, Coskran TM, Culp JS, James LC, Krull DL, Lanfear J, Ryan AM, Schmidt CJ, Strick CA, Varghese AH, Williams RD, Wylie PG, Menniti FS (2003) Immunohistochemical localization of PDE10A in the rat brain. Brain Res 985(2):113–126. https://doi.org/10.1016/s0006-8993(03)02754-9
8. Hebb AL, Robertson HA, Denovan-Wright EM (2004) Striatal phosphodiesterase mRNA and protein levels are reduced in Huntington's disease transgenic mice prior to the onset of motor symptoms. Neuroscience 123(4):967–981. https://doi.org/10.1016/j.neuroscience.2003.11.009
9. Giampa C, Laurenti D, Anzilotti S, Bernardi G, Menniti FS, Fusco FR (2010) Inhibition of the striatal specific phosphodiesterase PDE10A ameliorates striatal and cortical pathology in R6/2 mouse model of Huntington's disease. PLoS ONE 5(10):e13417. https://doi.org/10.1371/journal.pone.0013417
10. Lee YY, Park JS, Leem YH, Park JE, Kim DY, Choi YH, Park EM, Kang JL, Kim HS (2019) The phosphodiesterase 10 inhibitor papaverine exerts anti-inflammatory and neuroprotective effects via the PKA signaling pathway in neuroinflammation and Parkinson's disease mouse models. J Neuroinflammation 16(1):246. https://doi.org/10.1186/s12974-019-1649-3
11. Ito M, Aswendt M, Lee AG, Ishizaka S, Cao Z, Wang EH, Levy SL, Smerin DL, McNab JA, Zeineh M, Leuze C, Goubran M, Cheng MY, Steinberg GK (2018) RNA-sequencing analysis revealed a distinct motor cortex transcriptome in spontaneously recovered mice after stroke. Stroke 49(9):2191–2199. https://doi.org/10.1161/STROKEAHA.118.021508
12. Birjandi SZ, Abduljawad N, Nair S, Dehghani M, Suzuki K, Kimura H, Carmichael ST (2021) Phosphodiesterase 10A inhibition leads to brain region-specific recovery based on stroke type. Transl Stroke Res 12(2):303–315. https://doi.org/10.1007/s12975-020-00819-8
13. Suzuki K, Harada A, Suzuki H, Miyamoto M, Kimura H (2016) TAK-063, a PDE10A inhibitor with balanced activation of direct and indirect pathways, provides potent antipsychotic-like effects in multiple paradigms. Neuropsychopharmacology : official publication of the American College of Neuropsychopharmacology 41(9):2252–2262. https://doi.org/10.1038/npp.2016.20
14. Goldsmith P, Affinito J, McCue M, Tsai M, Roepcke S, Xie J, Gertsik L, Macek TA (2017) A Randomized multiple dose pharmacokinetic study of a novel PDE10A inhibitor TAK-063 in subjects with stable schizophrenia and Japanese subjects and modeling of exposure relationships to adverse events. Drugs R D 17(4):631–643. https://doi.org/10.1007/s40268-017-0214-8
15. Yurgelun-Todd DA, Renshaw PF, Goldsmith P, Uz T, Macek TA (2019) A randomized, placebo-controlled, phase 1 study to evaluate the effects of TAK-063 on ketamine-induced changes in fMRI BOLD signal in healthy subjects. Psychopharmacology. https://doi.org/10.1007/s00213-019-05366-1
16. Harada A, Suzuki K, Kamiguchi N, Miyamoto M, Tohyama K, Nakashima K, Taniguchi T, Kimura H (2015) Characterization of binding and inhibitory properties of TAK-063, a novel phosphodiesterase 10A inhibitor. PLoS ONE 10(3):e0122197. https://doi.org/10.1371/journal.pone.0122197
17. Suzuki K, Kimura H (2018) TAK-063, a novel PDE10A inhibitor with balanced activation of direct and indirect pathways, provides a unique opportunity for the treatment of schizophrenia. CNS Neurosci Ther 24(7):604–614. https://doi.org/10.1111/cns.12798
18. Kunitomo J, Yoshikawa M, Fushimi M, Kawada A, Quinn JF, Oki H, Kokubo H, Kondo M, Nakashima K, Kamiguchi N, Suzuki K, Kimura H, Taniguchi T (2014) Discovery of 1-[2-fluoro-4-(1H-pyrazol-1-yl)phenyl]-5-methoxy-3-(1-phenyl-1H-pyrazol-5-yl) pyri dazin-4(1H)-one (TAK-063), a highly potent, selective, and orally active phosphodiesterase 10A (PDE10A) inhibitor. J Med Chem 57(22):9627–9643. https://doi.org/10.1021/jm5013648
19. Beker MC, Caglayan AB, Kelestemur T, Caglayan B, Yalcin E, Yulug B, Kilic U, Hermann DM, Kilic E (2015) Effects of normobaric oxygen and melatonin on reperfusion injury: role of cerebral microcirculation. Oncotarget 6(31):30604–30614. https://doi.org/10.18632/oncotarget.5773
20. Caglayan AB, Beker MC, Caglayan B, Yalcin E, Caglayan A, Yulug B, Hanoglu L, Kutlu S, Doeppner TR, Hermann DM, Kilic E (2019) Acute and post-acute neuromodulation induces stroke recovery by promoting survival signaling, neurogenesis, and pyramidal tract plasticity. Front Cell Neurosci 13:144. https://doi.org/10.3389/fncel.2019.00144
21. Beker MC, Caglayan B, Caglayan AB, Kelestemur T, Yalcin E, Caglayan A, Kilic U, Baykal AT, Reiter RJ, Kilic E (2019) Interaction of melatonin and Bmal1 in the regulation of PI3K/AKT pathway components and cellular survival. Sci Rep 9(1):19082. https://doi.org/10.1038/s41598-019-55663-0
22. Wisniewski JR, Zougman A, Nagaraj N, Mann M (2009) Universal sample preparation method for proteome analysis. Nat Methods 6(5):359–362. https://doi.org/10.1038/nmeth.1322
23. Yalcin E, Beker MC, Turkseven S, Caglayan B, Gurel B, Kilic U, Caglayan AB, Kalkan R, Baykal AT, Kelestemur T, Kilic E (2019) Evidence that melatonin downregulates Nedd4-1 E3 ligase and its role in cellular survival. Toxicol Appl Pharmacol 379:114686. https://doi.org/10.1016/j.taap.2019.114686
24. Beker MC, Caglayan B, Yalcin E, Caglayan AB, Turkseven S, Gurel B, Kelestemur T, Sertel E, Sahin Z, Kutlu S, Kilic U, Baykal AT, Kilic E (2018) Time-of-Day dependent neuronal injury after ischemic stroke: implication of circadian clock transcriptional factor Bmal1 and survival kinase AKT. Mol Neurobiol 55(3):2565–2576. https://doi.org/10.1007/s12035-017-0524-4
25. Acioglu C, Mirabelli E, Baykal AT, Ni L, Ratnayake A, Heary RF, Elkabes S (2016) Toll like receptor 9 antagonism modulates spinal cord neuronal function and survival: direct versus astrocyte-mediated mechanisms. Brain Behav Immun 56:310–324. https://doi.org/10.1016/j.bbi.2016.03.027
26. Kilic E, Bahr M, Hermann DM (2001) Effects of recombinant tissue plasminogen activator after intraluminal thread occlusion in mice: role of hemodynamic alterations. Stroke 32(11):2641–2647. https://doi.org/10.1161/hs1101.097381
27. Bacigaluppi M, Pluchino S, Peruzzotti-Jametti L, Kilic E, Kilic U, Salani G, Brambilla E, West MJ, Comi G, Martino G, Hermann DM (2009) Delayed post-ischaemic neuroprotection following systemic neural stem cell transplantation involves multiple mechanisms. Brain 132(Pt 8):2239–2251. https://doi.org/10.1093/brain/awp174
28. Huan X, Oumei C, Hongmei Q, Junxia Y, Xiaojiao M, Qingsong J (2019) PDE9 inhibition promotes proliferation of neural stem cells via cGMP-PKG pathway following oxygen-glucose deprivation/reoxygenation injury in vitro. Neurochem Int 133:104630. https://doi.org/10.1016/j.neuint.2019.104630
29. Omori K, Kotera J (2007) Overview of PDEs and their regulation. Circ Res 100(3):309–327. https://doi.org/10.1161/01.RES.0000256354.95791.f1
30. Russwurm C, Koesling D, Russwurm M (2015) Phosphodiesterase 10A is tethered to a synaptic signaling complex in striatum. J Biol Chem 290(19):11936–11947. https://doi.org/10.1074/jbc.M114.595769
31. Tejeda GS, Whiteley EL, Deeb TZ, Burli RW, Moss SJ, Sheridan E, Brandon NJ, Baillie GS (2020) Chorea-related mutations in PDE10A result in aberrant compartmentalization and functionality of the enzyme. Proc Natl Acad Sci USA 117(1):677–688. https://doi.org/10.1073/pnas.1916398117
32. Knopp C, Hausler M, Muller B, Damen R, Stoppe A, Mull M, Elbracht M, Kurth I, Begemann M (2019) PDE10A mutation in two sisters with a hyperkinetic movement disorder—response to

levodopa. Parkinsonism Relat Disord 63:240–242. https://doi.org/10.1016/j.parkreldis.2019.02.007
33. VerPlank JJS, Tyrkalska SD, Fleming A, Rubinsztein DC, Goldberg AL (2020) cGMP via PKG activates 26S proteasomes and enhances degradation of proteins, including ones that cause neurodegenerative diseases. Proc Natl Acad Sci USA 117(25):14220–14230. https://doi.org/10.1073/pnas.2003277117
34. Zhang H, Pan B, Wu P, Parajuli N, Rekhter MD, Goldberg AL, Wang X (2019) PDE1 inhibition facilitates proteasomal degradation of misfolded proteins and protects against cardiac proteinopathy. Science advances 5(5):eaaw5870. https://doi.org/10.1126/sciadv.aaw5870
35. Myeku N, Duff KE (2018) Targeting the 26S proteasome to protect against proteotoxic diseases. Trends Mol Med 24(1):18–29. https://doi.org/10.1016/j.molmed.2017.11.006
36. Krueger M, Mages B, Hobusch C, Michalski D (2019) Endothelial edema precedes blood-brain barrier breakdown in early time points after experimental focal cerebral ischemia. Acta Neuropathol Commun 7(1):17. https://doi.org/10.1186/s40478-019-0671-0
37. Uzdensky AB (2020) Regulation of apoptosis in the ischemic penumbra in the first day post-stroke. Neural Regen Res 15(2):253–254. https://doi.org/10.4103/1673-5374.265546
38. Xing C, Arai K, Lo EH, Hommel M (2012) Pathophysiologic cascades in ischemic stroke. Int J Stroke 7(5):378–385. https://doi.org/10.1111/j.1747-4949.2012.00839.x
39. Dirnagl U, Kaplan B, Jacewicz M, Pulsinelli W (1989) Continuous measurement of cerebral cortical blood flow by laser-Doppler flowmetry in a rat stroke model. J. Cereb 9(5):589–596. https://doi.org/10.1038/jcbfm.1989.84
40. Hedna VS, Ansari S, Shahjouei S, Cai PY, Ahmad AS, Mocco J, Qureshi AI (2015) Validity of laser Doppler flowmetry in predicting outcome in murine intraluminal middle cerebral artery occlusion stroke. J Vasc Interv Neurol 8(3):74–82
41. Shi X, Wang J, Lei Y, Cong C, Tan D, Zhou X (2019) Research progress on the PI3K/AKT signaling pathway in gynecological cancer (Review). Mol Med Rep 19(6):4529–4535. https://doi.org/10.3892/mmr.2019.10121
42. Carracedo A, Pandolfi PP (2008) The PTEN-PI3K pathway: of feedbacks and cross-talks. Oncogene 27(41):5527–5541. https://doi.org/10.1038/onc.2008.247
43. Kilic U, Caglayan AB, Beker MC, Gunal MY, Caglayan B, Yalcin E, Kelestemur T, Gundogdu RZ, Yulug B, Yilmaz B, Kerman BE, Kilic E (2017) Particular phosphorylation of PI3K/Akt on Thr308 via PDK-1 and PTEN mediates melatonin's neuroprotective activity after focal cerebral ischemia in mice. Redox Biol 12:657–665. https://doi.org/10.1016/j.redox.2017.04.006
44. Gao X, Zhang H, Steinberg G, Zhao H (2010) The Akt pathway is involved in rapid ischemic tolerance in focal ischemia in rats. Transl Stroke Res 1(3):202–209. https://doi.org/10.1007/s12975-010-0017-5
45. LiCausi F, Hartman NW (2018) Role of mTOR complexes in neurogenesis. Int J Mol Sci 19(5):1544. https://doi.org/10.3390/ijms19051544
46. Amalia L, Sadeli HA, Parwati I, Rizal A, Panigoro R (2020) Hypoxia-inducible factor-1alpha in acute ischemic stroke: neuroprotection for better clinical outcome. Heliyon 6(6):e04286. https://doi.org/10.1016/j.heliyon.2020.e04286
47. Davis CK, Jain SA, Bae ON, Majid A, Rajanikant GK (2018) Hypoxia mimetic agents for ischemic stroke. Dev. Biol 6:175. https://doi.org/10.3389/fcell.2018.00175
48. Baranova O, Miranda LF, Pichiule P, Dragatsis I, Johnson RS, Chavez JC (2007) Neuron-specific inactivation of the hypoxia inducible factor 1 alpha increases brain injury in a mouse model of transient focal cerebral ischemia. J. Neurosci 27(23):6320–6332. https://doi.org/10.1523/JNEUROSCI.0449-07.2007
49. Jiang X, Andjelkovic AV, Zhu L, Yang T, Bennett MVL, Chen J, Keep RF, Shi Y (2018) Blood-brain barrier dysfunction and recovery after ischemic stroke. Prog Neurobiol 163–164:144–171. https://doi.org/10.1016/j.pneurobio.2017.10.001
50. Turner RJ, Sharp FR (2016) Implications of MMP9 for blood brain barrier disruption and hemorrhagic transformation following ischemic stroke. Front Cell Neurosci 10:56. https://doi.org/10.3389/fncel.2016.00056
51. D'Orsi B, Mateyka J, Prehn JHM (2017) Control of mitochondrial physiology and cell death by the Bcl-2 family proteins Bax and Bok. Neurochem Int 109:162–170. https://doi.org/10.1016/j.neuint.2017.03.010
52. Doll DN, Barr TL, Simpkins JW (2014) Cytokines: their role in stroke and potential use as biomarkers and therapeutic targets. Aging Dis 5(5):294–306. https://doi.org/10.14336/AD.2014.0500294
53. Li KW, Ganz AB, Smit AB (2019) Proteomics of neurodegenerative diseases: analysis of human post-mortem brain. J Neurochem 151(4):435–445. https://doi.org/10.1111/jnc.14603
54. Zhang X, Wang X, Khurm M, Zhan G, Zhang H, Ito Y, Guo Z (2020) Alterations of brain quantitative proteomics profiling revealed the molecular mechanisms of diosgenin against cerebral ischemia reperfusion effects. J Proteome Res 19(3):1154–1168. https://doi.org/10.1021/acs.jproteome.9b00667
55. Rodrigues-Amorim D, Rivera-Baltanas T, Vallejo-Curto MDC, Rodriguez-Jamardo C, de Las HE, Barreiro-Villar C, Blanco-Formoso M, Fernandez-Palleiro P, Alvarez-Ariza M, Lopez M, Garcia-Caballero A, Olivares JM, Spuch C (2019) Proteomics in schizophrenia: a gateway to discover potential biomarkers of psychoneuroimmune pathways. Front Psych 10:885. https://doi.org/10.3389/fpsyt.2019.00885